Face-sharing structure perovskite air electrodes with boosted oxygen diffusion and durability for reversible protonic ceramic cells

Jing Wang ,[a] Fanghan Zhao ,[a] Yitong Li ,[a] Chenghao Yang ,[a] Luyun Yang,*[b] Yuan Tan,*[c] Jian Pu[a] and Bo Chi*[a]

a School of Materials Science and Engineering, Huazhong University of Science and Technology, Wuhan 430074, China. Email: chibo@hust.edu.cn
b Wuhan National Laboratory for Optoelectronics, Huazhong University of Science and Technology, Wuhan 430074, China. Email: Luyunyang@gmail.com
c Engineering Research Center of Surface and Interface Regulation Technology and Equipment for Renewable Energy Materials, School of Optoelectronic Materials & Technologies, Jianghan University, Wuhan 430056, China. Email: tanyuan@jhun.edu.cn

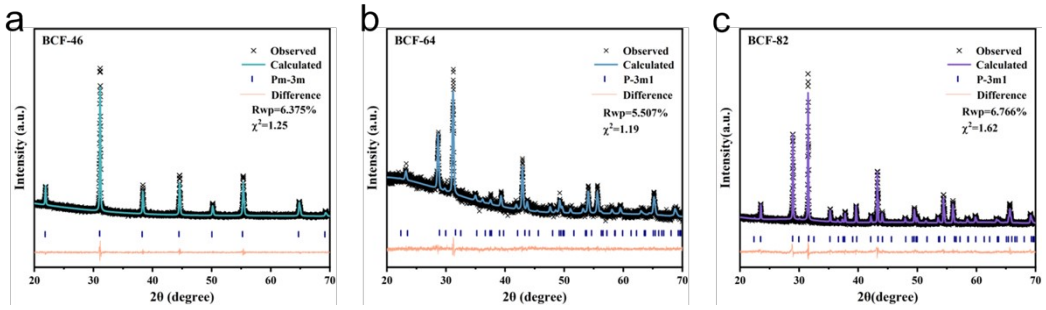

Figure S1. Refined XRD profile of (a) BCF46, (b) BCF64, (c) BCF82 powders.

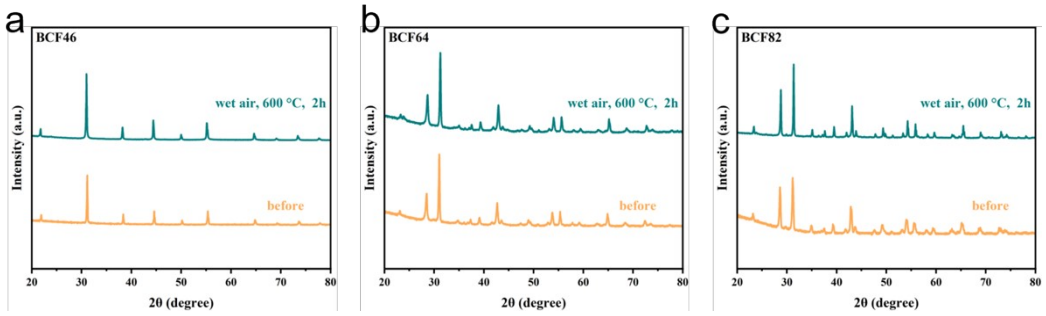

Figure S2. XRD patterns of the (a) BCF46, (b) BCF64, (c) BCF82 after exposed to wet air (2 h, 600 °C).

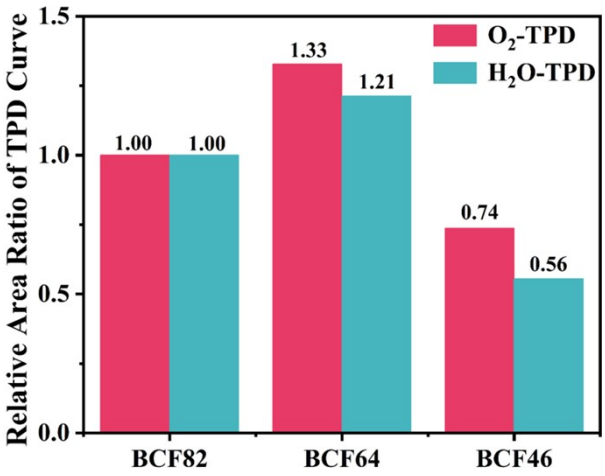

Figure S3. Relative area ratio of O_2-TPD and H_2O-TPD curves based on BCF82

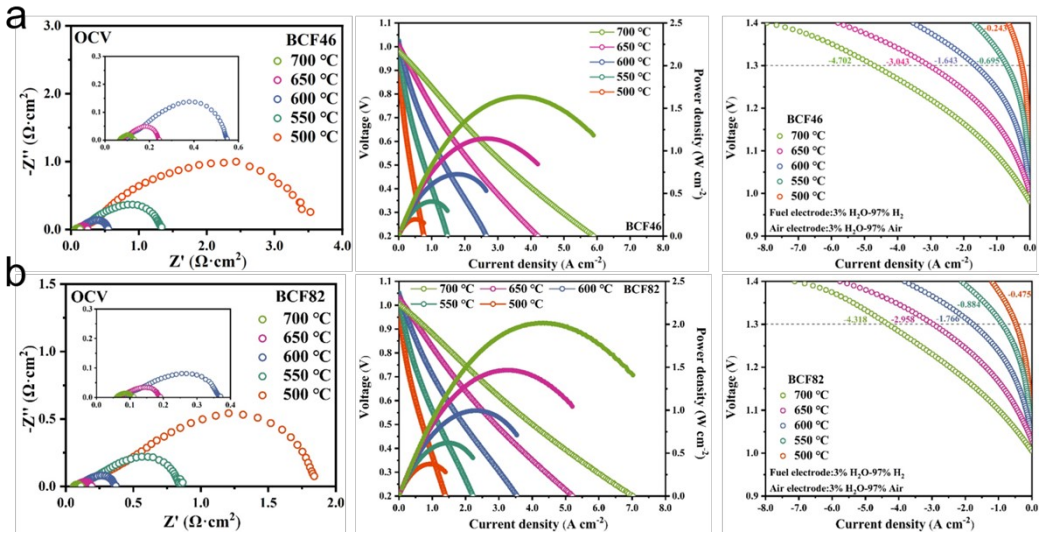

Figure S4. EIS, I-V-P and IV curves of single cells. (a) BCF46 and (b) BCF82.

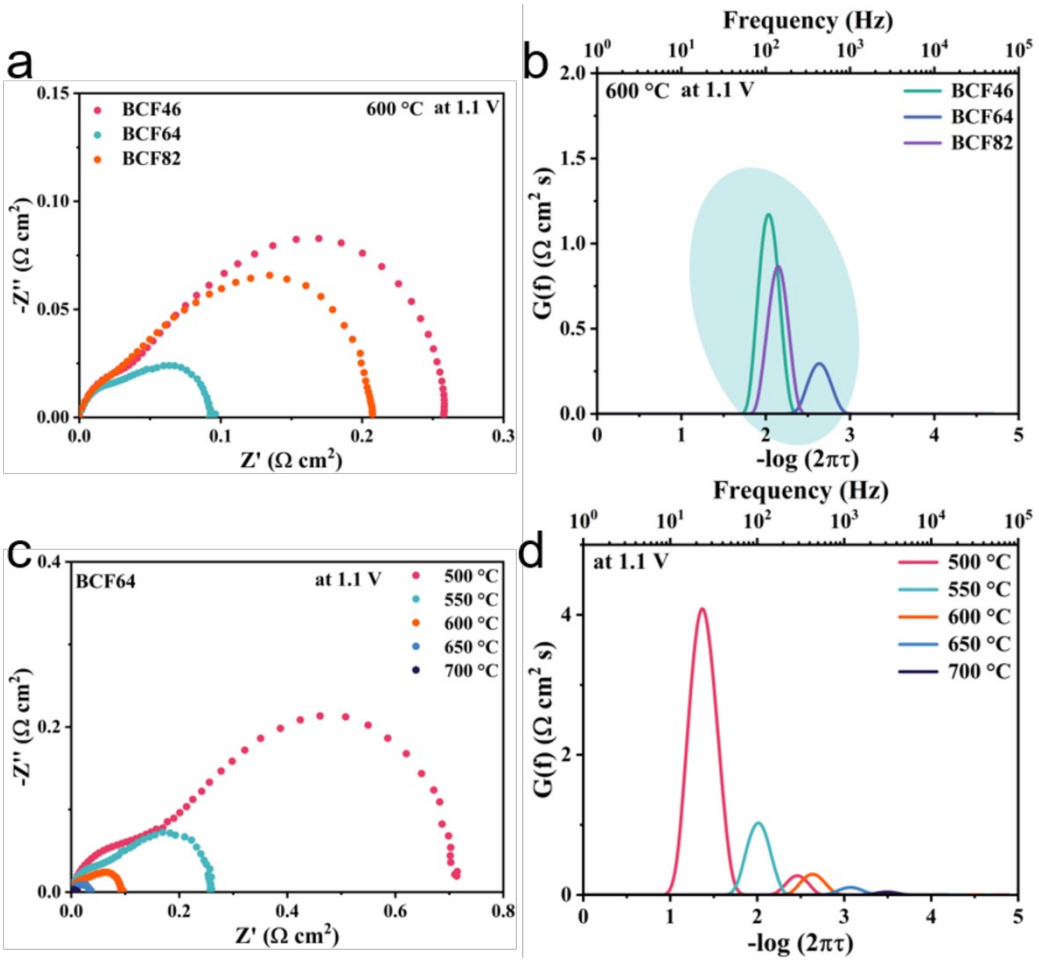

Figure S5. (a) Polarization impedance and (b) DRT analysis of three electrode materials at 600 °C and 1.1 V polarization voltage, and (c) polarization impedance and (d) DRT analysis of BCF64 at different temperatures under 1.1 V polarization voltage.

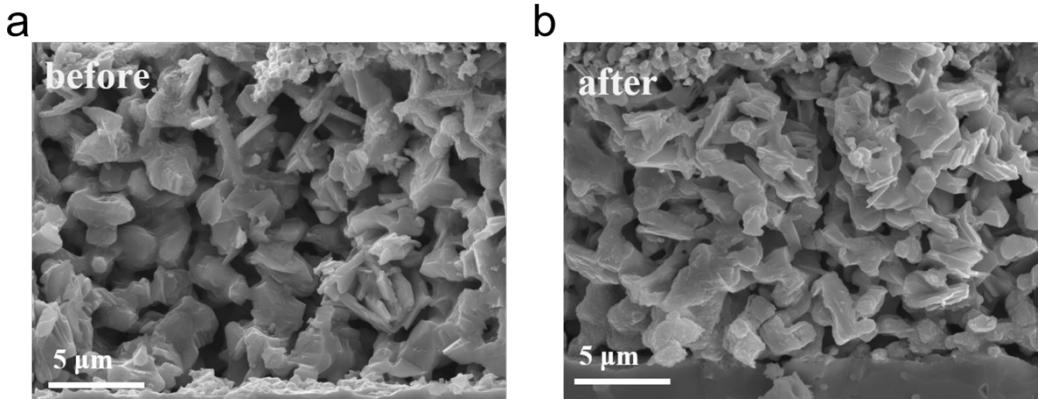

Figure S6. The electrode micromorphology of BCF64 (a) before and (b) after long-term test.

Table S1. XRD Refinement results for $BaCo_{1-x}Fe_xO_{3-\delta}$ (x = 0.2, 0.4, 0.6) electrodes.

Sample	χ^2	Space group	a(Å)	b(Å)	c(Å)	α	β	γ	3−δ
BCF46	1.25	Pm-3m	4.0662	4.0662	4.0662	90°	90°	90°	2.691
BCF64	1.19	P-3m1	5.7081	5.7081	11.9322	90°	90°	120°	2.644
BCF82	1.62	P-3m1	5.6599	5.6599	11.8594	90°	90°	120°	2.674

Table S2. The structural parameters of BCF46 obtained by Rietveld refinement.

Atom	x	y	z	Fraction
Ba1	0.000	0.000	0.000	1.000
Co1	0.500	0.500	0.500	0.390
O1	0.500	0.500	0.00	0.897
Fe1	0.500	0.500	0.500	0.610

Table S3. The structural parameters of BCF64 obtained by Rietveld refinement.

Atom	x	y	z	Fraction
Ba1	0.000	0.000	0.000	1.000
Ba2	0.333	0.667	0.768	1.000
Ba3	0.333	0.667	0.417	1.000
Co1	0.000	0.000	0.500	0.600
Co2	0.000	0.000	0.301	0.600
Co3	0.333	0.667	0.114	0.600
O1	0.333	0.667	0.002	0.994
O2	0.124	0.876	0.208	0.836
O3	0.175	0.825	0.582	0.889
Fe1	0.000	0.000	0.500	0.400
Fe2	0.000	0.000	0.249	0.400
Fe3	0.333	0.667	0.172	0.400

Table S4. The structural parameters of BCF82 obtained by Rietveld refinement.

Atom	x	y	z	Fraction
Ba1	0.000	0.000	0.000	1.000
Ba2	0.333	0.667	0.772	1.000
Ba3	0.333	0.667	0.417	1.000
Co1	0.000	0.000	0.500	0.800
Co2	0.000	0.000	0.306	0.850
Co3	0.333	0.667	0.130	0.764
O1	0.333	0.667	0.002	0.996
O2	0.168	0.832	0.187	0.856
O3	0.163	0.837	0.607	0.892
Fe1	0.000	0.000	0.500	0.200
Fe2	0.000	0.000	0.229	0.150
Fe3	0.333	0.667	0.178	0.236

Table S5. Analysis of spectra for $BaCo_{1-x}Fe_xO_{3-\delta}$ (x = 0.2, 0.4, 0.6) powders.

Sample	Element	Atomic Fraction(%)	Atomic Error(%)	Mass Fraction(%)	Mass Error(%)	Fit Fraction(%)
BCF46	Ba	14.05	1.33	49.12	2.91	0.09
	Co	6.08	0.77	9.12	1.22	0.31
	Fe	9.10	1.11	12.93	1.66	0.19
	O	70.77	1.50	28.82	1.66	0.36
BCF64	Ba	17.82	1.64	52.12	3.05	0.09
	Co	13.83	1.62	17.36	2.16	0.16
	Fe	8.51	1.06	10.12	1.36	0.15
	O	59.84	1.74	20.40	1.28	0.24
BCF82	Ba	17.70	1.63	53.07	3.08	0.03
	Co	15.45	1.77	19.88	2.41	0.05
	Fe	4.27	0.56	5.20	0.73	0.05
	O	62.57	1.81	21.85	1.41	0.97

Table S6. The Co 2p3/2 binding energy and content of Co^{4+} and Co^{3+} were calculated from the corresponding XPS peaks.

Sample	Co^{3+}(eV)	Co^{4+}(eV)	Co^{3+}(%)	Co^{4+} (%)	Average valence state
BCF46	778.76	781.20	75.42	24.58	+3.25
BCF64	778.74	781.40	75.03	24.97	+3.25
BCF82	778.98	781.22	73.22	26.78	+3.27

Table S7. The Fe 2p3/2 binding energy and content of Fe^{2+} and Fe^{3+} calculated from the corresponding XPS peaks.

Sample	Fe^{2+}(eV)	Fe^{3+}(eV)	Fe^{2+}(%)	Fe^{3+}(%)	Average valence state
BCF46	710.40	713.35	71.78	28.22	+2.28
BCF64	710.27	712.66	53.81	46.19	+2.46
BCF82	709.95	712.12	50.10	49.90	+2.50

Table S8. Comparison of the peak power densities (PPDs) of BCF64 single cell with other recently reported single cells which possess a similar construction.

Cell Structure	Atmosphere	Peak power density(W cm^{-2})				Reference
		500 °C	550 °C	600 °C	650 °C	
Ni-BZCYYb1711|BZCYYb1711|PBCC-BCO	H_2 (3% H_2O)/ Ambient air		0.66	1.06	1.58	[1]
Ni-BZCYYb1711|BZCYYb1711|BCFZY	H_2/Air	0.45	0.52	0.65		[2]
Ni-BZCYYb4411|BZCYYb4411|PBSCF(with PLD layer)	Humidified H_2/ Synthetic air	0.55	0.78	1.10	1.42	[3]
Ni-BZCYYb1711|BZCYYb1711|BCFT10	H_2 /Air(3% H_2O)	0.48	0.74	1.05	1.47	[4]
Ni-BZCYYb1711|BZCYYb1711|BCT20(with PLD layer)	H_2 (3% H_2O)/ Air	0.76	1.14	1.64	2.26	[5]
Ni-BZCYYb1711|BZCYYb1711|BCFZYN-095			0.54		1.04	[6]
Ni-BZCYYb1711|BZCYYb1711|NBSCF	H_2 (3% H_2O)/ Air			0.69	1.05	[7]
Ni-BZCYYb4411|BZCYYb4411|BSTC(with PLD layer)	H_2 (3% H_2O)/ Air (3% H_2O)	0.84	1.46	2.25	3.15	[8]
Ni-BZCYYb1711|BZCYYb1711|BCCY	H_2 / Ambient air	0.319	0.508	0.743	0.985	[9]
Ni-BZCYYb1711|BZCYYb1711|BC1.5MN	H_2 (3% H_2O)/ Air	0.34	0.54	0.84	1.17	[10]
Ni-BZCYYb1711|BZCYYb1711|BCFN	H_2 (3% H_2O)/ Ambient air	0.5	0.8	1.2	1.7	[11]
Ni-BZCYYb1711|BZCYYb1711|BSCFE0.1	H_2 / Air (10% H_2O)	0.525	0.701	0.984	1.327	[12]
Ni-BZCYYb1711|BZCYYb1711|BCF46	H_2 (3% H_2O)/ Ambient air	0.196	0.405	0.725	1.436	This work
Ni-BZCYYb1711|BZCYYb1711|BCF64	H_2 (3% H_2O)/ Ambient air	0.420	0.703	1.094	1.488	This work
Ni-BZCYYb1711|BZCYYb1711|BCF82	H_2 (3% H_2O)/ Ambient air	0.373	0.619	0.996	1.467	This work

Note: PBCC-BCO ($PrBa_{0.8}Ca_{0.2}Co_2O_{5+\delta}$), BCFZY ($BaCo_{0.4}Fe_{0.4}Zr_{0.1}Y_{0.1}O_{3-\delta}$), PBSCF ($PrBa_{0.5}Sr_{0.5}Co_{1.5}Fe_{0.5}O_{5+\delta}$), BCFT10 ($Ba(Co_{0.7}Fe_{0.3})_{0.9}Ta_{0.1}O_{3-\delta}$), BCT20 ($BaCo_{0.8}Ta_{0.2}O_{3-\delta}$), BCFZYN-095 ($Ba_{0.95}(Co_{0.4}Fe_{0.4}Zr_{0.1}Y_{0.1})_{0.95}Ni_{0.05}O_{3-\delta}$), NBSCF ($NdBa_{0.5}Sr_{0.5}Co_{1.5}Fe_{0.5}O_{5+\delta}$), BSTC($BaSc_{0.1}Ta_{0.1}Co_{0.8}O_{3-\delta}$), BCCY ($BaCo_{0.7}(Ce_{0.8}Y_{0.2})_{0.3}O_{3-\delta}$), BC1.5MN ($Ba_2Co_{1.5}Mo_{0.25}Nb_{0.25}O_{6-\delta}$), BCFN ($Ba_{0.9}Co_{0.7}Fe_{0.2}Nb_{0.1}O_{3-\delta}$), BSCFE0.1 ($Ba_{0.5}Sr_{0.5}(Co_{0.8}Fe_{0.2})_{0.9}Er_{0.1}O_{3-\delta}$).

Table S9. Comparison of the electrolytic current density of BCF64 single cell with other recently reported single cells which possess a similar construction.

Cell Structure	Atmosphere	Electrolytic current density (A cm^{-2}) at 1.3 V				Reference
		500 °C	550 °C	600 °C	650 °C	
Ni-BZCYYb1711|BZCYYb1711|PBCC-BCO	H_2 (3% H_2O)/ Air (3% H_2O)		0.69	1.51	2.52	[1]
Ni-BZCYYb1711|BZCYYb1711|BCFZY						[2]
Ni-BZCYYb4411|BZCYYb4411|PBSCF(with PLD layer)						[3]
Ni-BZCYYb1711|BZCYYb1711|BCFT10	H_2 /Air(3% H_2O)	0.55 (at 1.4 v)	1.00 (at 1.4 v)	1.65 (at 1.4 v)	2.11 (at 1.4 v)	[4]
Ni-BZCYYb1711|BZCYYb1711|BCT20(with PLD layer)	H_2 (3% H_2O)/ Air (3% H_2O)		0.84	1.60	2.33	[5]
Ni-BZCYYb1711|BZCYYb1711|BCFZYN-095						[6]
Ni-BZCYYb1711|BZCYYb1711|NBSCF						[7]
Ni-BZCYYb4411|BZCYYb4411|BSTC(with PLD layer)	H_2 (3% H_2O)/ Air (3% H_2O)	0.62	1.49	2.88	4.21	[8]
Ni-BZCYYb1711|BZCYYb1711|BCCY						[9]
Ni-BZCYYb1711|BZCYYb1711|BC1.5MN	H_2 (3% H_2O)/ Air (3% H_2O)		0.68	1.34	2.04	[10]
Ni-BZCYYb1711|BZCYYb1711|BCFN	H_2 (3% H_2O)/ Air (3% H_2O)	0.3	0.7	1.6	2.8	[11]
Ni-BZCYYb1711|BZCYYb1711|BSCFE0.1	H_2 / Air (10% H_2O)	0.564	1.046	1.535	2.227	[12]
Ni-BZCYYb1711|BZCYYb1711|BCF46	H_2 (3% H_2O)/ Air (3% H_2O)	0.196	0.405	0.725	1.436	This work
Ni-BZCYYb1711|BZCYYb1711|BCF64	H_2 (3% H_2O)/ Air (3% H_2O)	0.420	0.703	1.094	1.488	This work
Ni-BZCYYb1711|BZCYYb1711|BCF82	H_2 (3% H_2O)/ Air (3% H_2O)	0.373	0.619	0.996	1.467	This work

Note: PBCC-BCO ($PrBa_{0.8}Ca_{0.2}Co_2O_{5+\delta}$), BCFZY ($BaCo_{0.4}Fe_{0.4}Zr_{0.1}Y_{0.1}O_{3-\delta}$), PBSCF ($PrBa_{0.5}Sr_{0.5}Co_{1.5}Fe_{0.5}O_{5+\delta}$),

BCFT10 ($Ba(Co_{0.7}Fe_{0.3})_{0.9}Ta_{0.1}O_{3-\delta}$), BCT20 ($BaCo_{0.8}Ta_{0.2}O_{3-\delta}$), BCFZYN-095 ($Ba_{0.95}(Co_{0.4}Fe_{0.4}Zr_{0.1}Y_{0.1})_{0.95}Ni_{0.05}O_{3-\delta}$), NBSCF ($NdBa_{0.5}Sr_{0.5}Co_{1.5}Fe_{0.5}O_{5+\delta}$), BSTC($BaSc_{0.1}Ta_{0.1}Co_{0.8}O_{3-\delta}$), BCCY ($BaCo_{0.7}(Ce_{0.8}Y_{0.2})_{0.3}O_{3-\delta}$), BC1.5MN ($Ba_2Co_{1.5}Mo_{0.25}Nb_{0.25}O_{6-\delta}$), BCFN ($Ba_{0.9}Co_{0.7}Fe_{0.2}Nb_{0.1}O_{3-\delta}$), BSCFE0.1 ($Ba_{0.5}Sr_{0.5}(Co_{0.8}Fe_{0.2})_{0.9}Er_{0.1}O_{3-\delta}$).

References

1 Y. Zhou, E. Liu, Y. Chen, Y. Liu, L. Zhang, W. Zhang, Z. Luo, N. Kane, B. Zhao, L. Soule, Y. Niu, Y. Ding, H. Ding, D. Ding, M. Liu*, ACS Energy Lett.*, 2021, 6, 1511-1520

2 C. Duan, J. Tong, M. Shang, S. Nikodemski, M. Sanders, S. Ricote, A. Almansoori, R. O'Hayre*, Science*, 2015, 349, 1321-1326

3 S. Choi, C. J. Kucharczyk, Y. Liang, X. Zhang, I. Takeuchi, H. Ji, S. M. Haile*, Nat. Energy*, 2018, 3, 202-210

4 Y. Feng, Y. Shen, F. Wang, C. Tian, Q. Hu, Q. Duan, J. Li, D. Bao*, Rare Metals*, 2024, 43, 3055-3065

5 J. H. Kim, D. Kim, S. Ahn, K. J. Kim, S. Jeon, D. Lim, J. K. Kim, U. Kim, H. Im, B. Koo, K. T. Lee, W. Jung*, Energy Environ. Sci.*, 2023, 16, 3803-3814

6 M. Liang, Y. Zhu, Y. Song, D. Guan, Z. Luo, G. Yang, S. P. Jiang, W. Zhou, R. Ran, Z. Shao*, Adv. Mater.*, 2022, 34, 2106379

7 J. Kim, S. Sengodan, G. Kwon, D. Ding, J. Shin, M. Liu, G. Kim*, ChemSusChem*, 2014, 7, 2811-2815

8 D. Kim, I. Jeong, S. Ahn, S. Oh, H. Im, H. Bae, S. J. Song, C. Lee, W. Jung, K. T. Lee*, Adv. Energy Mater.*, 2024, 14, 2304059

9 Y. Song, Y. Chen, W. Wang, C. Zhou, Y. Zhong, G. Yang, W. Zhou, M. Liu, Z. Shao*, Joule*, 2019, 3, 2842-2853

10 F. He, S. Liu, T. Wu, M. Yang, W. Li, G. Yang, F. Zhu, H. Zhang, K. Pei, Y. Chen, W. Zhou, Z. Shao*, Adv. Funct. Mater.*, 2022, 32, 2206756

11 K. Pei, Y. Zhou, K. Xu, H. Zhang, Y. Ding, B. Zhao, W. Yuan, K. Sasaki, Y. Choi, Y. Chen, M. Liu*, Nat. Commun.*, 2022, 13, 2207

12 Z. Liu, Y. Lin, H. Nie, D. Liu, Y. Li, X. Zhao, T. Li, G. Yang, Y. Sun, Y. Zhu, W. Wang, R. Ran, W. Zhou, Z. Shao*, Adv. Funct. Mater.*, 2024, 34, 2311140